

# Stochastic Finite Element Modelling of Human Middle Ear

Arash Ebrahimi<sup>1</sup>, Nima Maftoon<sup>1</sup>

<sup>1</sup> Department of Systems Design Engineering, University of Waterloo, Waterloo, Canada

**Abstract**— Modelling the mechanics of the middle ear is important as it can extend our knowledge about the hearing process and enable us to develop new devices for the treatment and diagnosis of hearing disabilities. Most of the works in the literature of the modelling of middle-ear mechanics are focused on deterministic models. These models cannot consider the variability of input parameters that can happen due to the stochastic nature of the mechanical properties of tissues and variability between individuals. Stochastic models can consider the variability in the parameters and make us able to have more realistic representations of the physiology. In this work, we present a stochastic Finite Element Method (FEM) model of the human middle ear. We considered uncertainty in all mechanical properties and some geometrical properties of the middle-ear model and studied the effects of these uncertainties on the uncertainties of the outputs of the model.

**Keywords**— Human middle-ear Model, Stochastic finite element method, Uncertainty analysis.

## I. INTRODUCTION

The middle ear plays an important role in the hearing process by converting the acoustic stimuli in the ear canal to vibrations and transmitting these vibrations to the inner ear. Middle-ear models can be used for different purposes such as developing surgical simulators and simulating the response of the ear to pathological changes. Hence, researchers have used a variety of methods to model the middle-ear mechanics.

Some of the works in the literature are based on lumped parameter models of the middle ear [1]–[3]. One of the problems of the lumped models is that they cannot provide details of the motions in the middle ear. Therefore, many researchers have proposed models that are based on continuum mechanics. FEM is one of the continuum-mechanics-based models that has been extensively used to model middle-ear mechanics [4]. FEM can deal with complex geometries, material properties, and boundary conditions.

All of the middle-ear models in the literature are deterministic, but in reality model parameters have probabilistic distributions. These uncertainties can arise from our lack of knowledge (epistemic uncertainty) [5], or from the intrinsic natural variability of the input parameters due to the probabilistic distribution of the mechanical and geometrical prop-

erties of the structures in the middle ear (aleatory uncertainty) [6]. The effect of the latter can be seen in the variability of the physiologic measurements of the human ear in different individuals in the normative study of Whittemore et al. [7].

In this work, we present a stochastic FEM model of the middle ear that takes into account the variability of the mechanical properties of all structures in our model as well as the thickness of the tympanic membrane (TM).

## II. MATERIALS AND METHODS

### A. Geometry reconstruction and mesh

The reconstructed geometry of the middle ear is shown in Figure 1. The geometry was created based on the segmentation of a  $\mu$ CT image dataset of a 73-year-old male cadaver temporal bone. The scan was done using Xradia MicroXCT-200 at 90 kv and 8 W. This led to a dataset of  $1024 \times 1012 \times 1014$  cubic voxels with an isotropic voxel size of  $18.0828 \mu\text{m}$ . We used 3D slicer<sup>1</sup> software for the segmentation and creating the mesh. The segmentation process started by cropping the middle-ear region. We then used both automatic and manual segmentation techniques to segment the structures inside the middle ear. After finalizing segmenting all parts, we used the Segment Mesher toolbox of the 3D slicer to create a conformal mesh for all components of the model. We created a volumetric mesh (four-node tetrahedral elements) for all components except the tympanic membrane for which we created a mesh with shell elements (three-node triangular elements). A mesh convergence study was performed by increasing the number of tetrahedral elements by a factor of eight and the number of triangular elements by a factor of four. We compared the results in 400 equally spaced frequencies in the range of 100 Hz to 10 kHz and observed a maximum difference of 2.68 dB between the results obtained from the original mesh and the refined mesh for the umbo displacement amplitude. The size of elements was not uniform and the generated mesh had coarse elements in the

---

<sup>1</sup> <https://www.slicer.org/>

regions that do not have considerable deformation (such as ossicles).

### B. Deterministic FEM model

We used Code\_Aster<sup>2</sup> 14.4.0 open-source FEM package for our calculations. Code\_Aster is an extensively validated FEM solver [8] and has been used in the area of middle-ear mechanics [9], [10]. The ossicles, joints, and ligaments were modeled using 3D solid elements and the TM was modeled using Discrete Kirchhoff Theory (DKT) elements [11]. Our outputs of interest are the displacement frequency response function of the umbo and stapes footplate. The motion of the umbo is important as it is in the central part of TM that is also connected to the manubrium and the motion of the stapes footplate is important as it is the vibration output of the middle ear that is conveyed to the inner ear. Also, the transfer function of the middle ear can be found using the displacement information of the umbo and stapes footplate.

The mechanical properties of all structures of the baseline model are presented in Table 1. The references for the values of density and Young's modulus are presented in this table. We assumed all materials to be elastic and isotropic. Moreover, we modeled all soft tissues as nearly incompressible materials with a Poisson's ratio of 0.49 [9]. A Poisson's ratio of 0.3 was used for the ossicles [12]. We considered a cochlear impedance of 20 GΩ [12] in order to model the cochlear load. We also considered the surface area of the stapes footplate to be 2.3 mm<sup>2</sup> [10]. From these values, we calculated a viscous damping value of 0.1058 Ns/m for rep-

resenting the cochlear load. We considered this load to be uniformly distributed among 4 dashpots attached to the stapes footplate in the direction parallel to the piston-like motion. It should be noted that we compared the results of the baseline model (using stapes footplate area of 2.3 mm<sup>2</sup>) with the results obtained using the stapes footplate area from our 3-D model (3.6 mm<sup>2</sup>) and observed less than 1.5 dB difference in the magnitude of responses at all frequencies in the range of 100 Hz to 10 kHz. Furthermore, we used Rayleigh damping for all components of our model. The coefficients of Rayleigh damping of each structure are reported in Table 1. These coefficients were found by manually adjusting them to closely replicate the experimental measurement results of Voss et al. [17]. The thickness of the TM was also considered to be 74 μm [12].

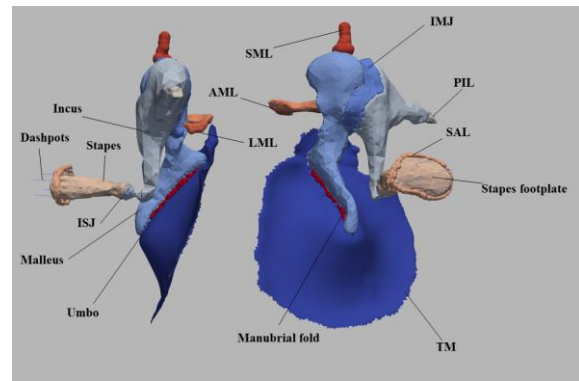


Fig. 1 Reconstructed geometry of the middle ear.

Table 1 Material Properties of the baseline model

| Structure                        | E (MPa)            | Density ( $kg/m^3$ ) | Poisson's ratio | $\alpha_1^3$ (1/s) | $\alpha_2^4$ (s)    |
|----------------------------------|--------------------|----------------------|-----------------|--------------------|---------------------|
| TM                               | 10 <sup>6</sup>    | 1200 <sup>6</sup>    | 0.49            | 700                | $4 \times 10^{-6}$  |
| Malleus                          | 14000 <sup>7</sup> | 2390 <sup>7</sup>    | 0.3             | 0                  | $4 \times 10^{-7}$  |
| Incus                            | 14000 <sup>7</sup> | 2150 <sup>7</sup>    | 0.3             | 0                  | $4 \times 10^{-7}$  |
| Stapes                           | 14000 <sup>7</sup> | 2200 <sup>7</sup>    | 0.3             | 0                  | $4 \times 10^{-7}$  |
| IMJ (incudomalleal joint)        | 30 <sup>7</sup>    | 1100 <sup>7</sup>    | 0.49            | 0                  | $13 \times 10^{-5}$ |
| ISJ (incudostapedial joint)      | 30 <sup>7</sup>    | 1100 <sup>7</sup>    | 0.49            | 0                  | $13 \times 10^{-5}$ |
| SAL (stapedial annular ligament) | 0.7 <sup>8</sup>   | 1200 <sup>7</sup>    | 0.49            | 0                  | $13 \times 10^{-5}$ |
| PIL (posterior incudal ligament) | 2 <sup>7</sup>     | 1200 <sup>7</sup>    | 0.49            | 700                | $4 \times 10^{-6}$  |
| LML (lateral malleal ligament)   | 2 <sup>7</sup>     | 1200 <sup>7</sup>    | 0.49            | 0                  | $13 \times 10^{-5}$ |
| Manubrial fold                   | 1 <sup>6</sup>     | 1200 <sup>6</sup>    | 0.49            | 700                | $4 \times 10^{-6}$  |
| SML (superior malleal ligament)  | 4.9 <sup>5</sup>   | 1200 <sup>9</sup>    | 0.49            | 0                  | $13 \times 10^{-5}$ |
| AML (anterior malleal ligament)  | 2 <sup>7</sup>     | 1200 <sup>7</sup>    | 0.49            | 0                  | $13 \times 10^{-5}$ |

<sup>3</sup> Rayleigh damping coefficient of mass

<sup>8</sup> Reference [15]

<sup>4</sup> Rayleigh damping coefficient of stiffness

<sup>9</sup> Reference [16]

<sup>5</sup> Reference [12]

<sup>6</sup> Reference [13]

<sup>7</sup> Reference [14]

<sup>2</sup> <https://www.code-aster.org/>

The TM annular region was considered to be fully clamped. The parts of the AML, LML, SML, PIL, and SAL that are in contact with the middle-ear cavity wall were considered to be clamped as well. The model was excited by the acoustic pressure uniformly applied to the entire TM area laterally.

### C. Propagating uncertainty

We considered uncertainty in the mechanical properties (i.e. Young's modulus, damping coefficients, and Poisson's ratio) of all components of the model as well as the thickness of the TM and the cochlear load. For all components of the model, we assumed normal distribution, which is advocated to be a suitable distribution for many biological variables [18]. We used the values reported in Table 1 for the deterministic baseline model as the mean values for creating stochastic sets of inputs. It should be noted that for the components with a Poisson's ratio of 0.49, we used half-normal distributions to generate values smaller than 0.49. The Coefficient of Variation (CoV), which is defined as the standard deviation divided by the mean, of all uncertain input components was considered to be 15%. The stochastic sets of inputs were created with the Latin Hypercube Sampling method with UQLab (version 1.3.0) [19] in MATLAB (version 2019a).

We performed 1960 model evaluations on the Niagara cluster of Compute Canada<sup>10</sup> with Intel Skylake (2.4 GHz, AVX512) processors running under the CentOS 7 distribution of Linux.

## III. RESULTS AND DISCUSSIONS

The calculated stochastic frequency response function of the umbo displacement is provided in Figure 2. In this figure, the mean value of all calculations, the results of the deterministic baseline model, the results of the stochastic simulations (gray thin lines), and the CoV of the stochastic response (as a measure of variability) are presented. The CoV of the umbo magnitude response has a small value at frequencies below 1000 Hz ( $\approx 10\%$ ) and reaches its maximum ( $\approx 48\%$ ) at about 2700 Hz. The CoV of the umbo phase response is small for frequencies below 1000Hz (with an average absolute value of about 17%) and the maximum absolute value of CoV happens near 1400 Hz ( $\approx 30\%$ ). From this figure, we can see that for some of the sets of inputs there is an anti-resonance near 2400 Hz. These anti-resonances can be detected in the phase responses as well.

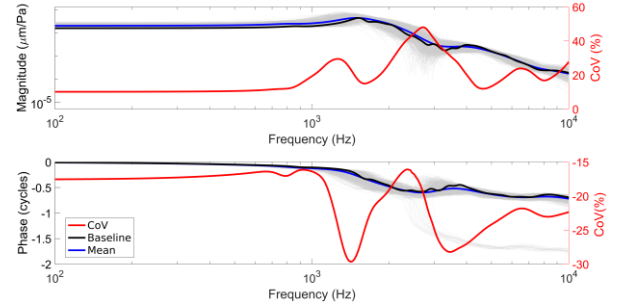


Fig. 2 Stochastic frequency response function of the umbo displacement. The results of stochastic simulations are presented with gray lines.

Figure 3 presents the stochastic results, mean value, results of the baseline model, and the CoV for the stapes footplate displacement. The experimental results of the measurements of Voss et al. are presented in this figure as well [17]. It should be mentioned that the original results presented by Voss et al. were in terms of velocity and we converted them to displacement.

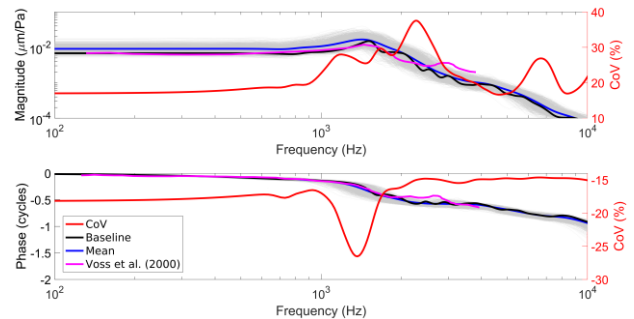


Fig. 3 Stochastic frequency response function of the stapes footplate displacement. The results of stochastic simulations are presented with gray lines.

Furthermore, the results presented by Voss et al. are uncorrected but they have reported a viewing angle (angle between a perpendicular to the stapes footplate and the measurement laser beam) of 20-50 degrees. We considered the viewing angle to be 35 degrees and used this value to correct the experimental data of Voss et al. shown in Figure 3 [17]. We compared the results of the amplitude of the baseline model with experimental results of Voss et al. at 150 frequencies (covering the entire frequency measurement range) and found that for 99 frequencies the difference was less than 1 dB and the maximum difference was 8.32 dB.

The results of Figure 3 show that similar to umbo response, the absolute value of CoV is small for both magnitude and phase at frequencies below 1000 Hz (about 17% for both magnitude and phase). For the magnitude, the maximum CoV happens at about 2270 Hz ( $\approx 37\%$ ) and for the phase, the maximum absolute value of CoV happens near

<sup>10</sup> <https://docs.computeCanada.ca/wiki/Niagara>

1400 Hz ( $\approx 26\%$ ). Also, the CoV for the phase of the stapes footplate has a small value at frequencies above 2000Hz (with an absolute value of about 14%) indicating a low variability at those frequencies.

#### IV. CONCLUSIONS

In this work, we presented a stochastic FEM model of the human middle ear. The main advantage of our stochastic model is its ability to predict the responses of the middle ear considering the natural variability in all mechanical properties of the middle-ear structures and the thickness of the TM. The calculated results of the frequency response of the displacement of the umbo and stapes footplate show that the maximum variation happens in the frequency range of 1 to 4 kHz. This model was validated with the experimental data from the literature but it was generated using a single cadaveric anatomy. Geometrical and pathological variability should be investigated in subsequent studies.

#### ACKNOWLEDGMENT

This work was supported by the Natural Sciences and Engineering Research Council of Canada (NSERC).

#### CONFLICT OF INTEREST

The authors declare that they have no conflict of interest.

#### REFERENCES

- [1] P. Parent and J. B. Allen, "Wave model of the cat tympanic membrane," *The Journal of the Acoustical Society of America*, vol. 122, no. 2, pp. 918–931, Aug. 2007, doi: 10.1121/1.2747156.
- [2] H. Hudde and C. Weistenhofer, "Circuit models of middle ear function," in *Rosowski, J. J., Merchant, S. N. (Eds.) The function and mechanics of normal, diseased and reconstructed middle ears*, Kugler Publications, pp. 39–58.
- [3] J. Zwislocki, "Analysis of the Middle-Ear Function. Part I: Input Impedance," *The Journal of the Acoustical Society of America*, vol. 34, no. 9B, pp. 1514–1523, Sep. 1962, doi: 10.1121/1.1918382.
- [4] W. R. J. Funnell, N. Maftoon, and W. F. Decraemer, "Modeling of Middle Ear Mechanics," in *The Middle Ear: Science, Otolaryngology, and Technology*, S. Puria, R. R. Fay, and A. N. Popper, Eds. New York, NY: Springer, 2013, pp. 171–210.
- [5] N. Mangado, G. Piella, J. Noailly, J. Pons-Prats, and M. Á. G. Ballester, "Analysis of Uncertainty and Variability in Finite Element Computational Models for Biomedical Engineering: Characterization and Propagation," *Front. Bioeng. Biotechnol.*, vol. 4, 2016, doi: 10.3389/fbioe.2016.00085.
- [6] C. J. Roy and W. L. Oberkampf, "A comprehensive framework for verification, validation, and uncertainty quantification in scientific computing," *Computer Methods in Applied Mechanics and Engineering*, vol. 200, no. 25–28, pp. 2131–2144, Jun. 2011, doi: 10.1016/j.cma.2011.03.016.
- [7] K. R. Whittemore, S. N. Merchant, B. B. Poon, and J. J. Rosowski, "A normative study of tympanic membrane motion in humans using a laser Doppler vibrometer (LDV)," *Hearing Research*, vol. 187, no. 1, pp. 85–104, Jan. 2004, doi: 10.1016/S0378-5955(03)00332-0.
- [8] D. Josselin, "Ranking of the documentation of Validation," [Online]. Available: [https://www.codeaster.org/V2/doc/v12/en/man\\_v/v0/v0.00.00.pdf](https://www.codeaster.org/V2/doc/v12/en/man_v/v0/v0.00.00.pdf).
- [9] N. Maftoon, W. R. J. Funnell, S. J. Daniel, and W. F. Decraemer, "Finite-element Modelling of the Response of the Gerbil Middle Ear to Sound," *Journal of the Association for Research in Otolaryngology*, vol. 16, no. 5, pp. 547–567, Oct. 2015, doi: 10.1007/s10162-015-0531-y.
- [10] H. Motallebzadeh, N. Maftoon, J. Pitaro, W. R. J. Funnell, and S. J. Daniel, "Finite-Element Modelling of the Acoustic Input Admittance of the Newborn Ear Canal and Middle Ear," *Journal of the Association for Research in Otolaryngology*, vol. 18, no. 1, pp. 25–48, Feb. 2017, doi: 10.1007/s10162-016-0587-3.
- [11] K.-J. Bathe and L.-W. Ho, "A simple and effective element for analysis of general shell structures," *Computers & Structures*, vol. 13, no. 5, pp. 673–681, Oct. 1981, doi: 10.1016/0045-7949(81)90029-8.
- [12] R. Z. Gan, B. Feng, and Q. Sun, "Three-dimensional finite element modeling of human ear for sound transmission," *Ann Biomed Eng.*, vol. 32, no. 6, pp. 847–859, Jun. 2004, doi: 10.1023/b:abme.0000030260.22737.53.
- [13] D. De Greef *et al.*, "Viscoelastic properties of the human tympanic membrane studied with stroboscopic holography and finite element modeling," *Hearing Research*, vol. 312, pp. 69–80, Jun. 2014, doi: 10.1016/j.heares.2014.03.002.
- [14] K. N. O'Connor, H. Cai, and S. Puria, "The effects of varying tympanic-membrane material properties on human middle-ear sound transmission in a three-dimensional finite-element model," *The Journal of the Acoustical Society of America*, vol. 142, no. 5, pp. 2836–2853, Nov. 2017, doi: 10.1121/1.5008741.
- [15] X. Zhang and R. Z. Gan, "Dynamic Properties of Human Stapedial Annular Ligament Measured With Frequency–Temperature Superposition," *J Biomech Eng.*, vol. 136, no. 8, pp. 0810041–0810047, Aug. 2014, doi: 10.1115/1.4027668.
- [16] K. Homma, Y. Shimizu, N. Kim, Y. Du, and S. Puria, "Effects of ear-canal pressurization on middle-ear bone- and air-conduction responses," *Hear Res*, vol. 263, no. 0, pp. 204–215, May 2010, doi: 10.1016/j.heares.2009.11.013.
- [17] S. E. Voss, J. J. Rosowski, S. N. Merchant, and W. T. Peake, "Acoustic responses of the human middle ear," *Hearing Research*, vol. 150, no. 1–2, pp. 43–69, Dec. 2000, doi: 10.1016/S0378-5955(00)00177-5.
- [18] G. L. Pearce and D. D. Frisbie, "Statistical evaluation of biomedical studies," *Osteoarthritis and Cartilage*, vol. 18, pp. S117–S122, Oct. 2010, doi: 10.1016/j.joca.2010.04.014.
- [19] S. Marelli and B. Sudret, "UQLab: A Framework for Uncertainty Quantification in Matlab," in *Vulnerability, Uncertainty, and Risk*, Liverpool, UK, Jun. 2014, pp. 2554–2563, doi: 10.1061/9780784413609.257.

Corresponding Author: Nima Maftoon  
 Institute: University of Waterloo  
 Street: 200 University Ave W  
 City: Waterloo  
 Country: Canada  
 Email: nmaftoon@uwaterloo.ca